JOURNAL OF CATALYSIS **159,** 219–229 (1996)
ARTICLE NO. 0081

W-Incorporated CoMo/γ-Al_2O_3 Hydrodesulfurization Catalyst

II. Characterization

Deuk Ki Lee,*[,1] Ho Tae Lee,* In Chul Lee,* Sung Koon Park,† Seong Youl Bae,†
Choong Hyon Kim,‡ and Seong Ihl Woo‡

*Energy Conversion Division, Korea Institute of Energy Research, Taedok Science Town, Taejon 305-343, Korea; †Department of Chemical Engineering, Hanyang University, Sung Dong Ku, Seoul 133-070, Korea; and ‡Department of Chemical Engineering, Korea Advanced Institute of Science & Technology, Taedok Science Town, Taejon 305-701, Korea

Received May 31, 1995; revised September 22, 1995; accepted October 9, 1995

Series of W-incorporated CoMo/γ-Al_2O_3 catalysts were characterized with TPR, DRS, ESR, and XPS. Two series of catalysts with varying content of tungsten were prepared for characterization by changing the impregnation order of cobalt and tungsten to a base Mo/γ-Al_2O_3 catalyst. The activity promotion by relatively low content of tungsten arose from the roles of tungsten in changing the Mo-oxide coordination from tetrahedral to octahedral, facilitating the reduction of Mo-oxide species, and increasing the dispersion of MoS_2. By incorporation of tungsten at a content as much as 0.025 in W/(W + Mo) atomic ratio, the MoS_2 dispersion of CoMo/γ-Al_2O_3 catalyst was considered to be maximized without noticible detriment to the active Co–Mo–O phase, resulting in the maximum activity promotion. The formation of the Co–Mo–O phases was more favored in the catalysts prepared by impregnating W onto CoMo/γ-Al_2O_3 than in those by impregnating W onto Mo/γ-Al_2O_3 before impregnation of Co. The effect of tungsten on the dispersion of active phase was not discriminated between the two series of catalysts. The activity decrease observed in the catalysts containing higher content of tungsten originated from the increase in the W-oxide coverage on the surface of Mo-oxides or Co–Mo–O phases, resulting in not only impeding the reduction or sulfidation of the oxidic precursor but facilitating the formation of less active Co–W–O at the sacrifice of more active Co–Mo–O phase.

INTRODUCTION

In the preceding paper (1), we reported that hydrodesulfurization (HDS) and hydrogenation (HYD) activities of the W-incorporated CoMo/γ-Al_2O_3 catalysts were promoted or decreased, depending on their tungsten composition. It was also found that the maximum activity promotion occurred at a low content of tungsten corresponding to 0.025 in W/(W + Mo) atomic ratio regardless of the impregnation order of tungsten. Adequate amounts of tungsten species present in CoMo/γ-Al_2O_3 catalyst can be considered to play a promoting role. As to the roles of conventional promoters such as nickel, cobalt, phosphorous, and fluoride, a number of possible promotion mechanism have been suggested as discussed by Prins *et al*. (2). As far as the alumina-supported HDS catalysts are concerned, the roles of promoters as a textural modifier and/or a bonding modifier of the active catalytic component have been significantly considered.

In this paper, as an extention of the previous study (1), W-incorporated CoMo/γ-Al_2O_3 was characterized to understand how the added tungsten species promoted the catalytic activity. The physicochemical properties of the catalysts in both the oxidic and sulfided states were investigated by means of X-ray diffraction (XRD), temperature-programmed reduction (TPR), diffuse reflectance spectroscopy (DRS), electron spin resonance spectroscopy (ESR), and X-ray photoelectron spectroscopy (XPS). The characterization results were discussed in relation to the catalytic activities in both HDS and HYD reactions.

EXPERIMENTAL

Catalysts

Catalysts for this study were the same as those used in the part I of this work (1), where their preparation details can be found. Series of catalysts denoted as CWM were prepared by impregnating tungsten onto the base catalyst of Mo(4.0) prior to impregnation of cobalt. The other series of catalyst, denoted as WCM, were obtained from tungsten impregnation onto Co(1.71)Mo(4.0) base. The two additional WCM catalysts which are equivalent to each other in their total metal content but different in their W/(W + Mo) atomic ratios have been prepared from their respective base catalysts, Co(2.14)Mo(4.87) and Co(2.14)Mo(4.0). These additional WCM catalysts, denoted as WCM-A, of

[1] To whom correspondence should be addressed.

0021-9517/96 $18.00

W(0.12)Co(2.14)Mo(4.87) and W(1.0)Co(2.14)Mo(4.0) are nearly same in their total metal loadings but have different W/(W + Mo) atomic ratios, 0.025 and 0.2, respectively. The numbers in parentheses following each catalytic component indicate the number of atoms per square nm of the surface area of alumina. The physical properties, the catalytic activities in thiophene HDS and ethylene HYD, and the O_2 uptake in the sulfided state of the prepared catalysts have been determined in the preceding part I (1).

XRD

An X-ray diffractometer (Rigaku) equipped with a Cu X-ray tube was used to obtain the diffraction patterns of the calcined catalyst samples.

TPR

The temperature-programmed reduction (TPR) experiments were carried out in the same apparatus used for HDS and HYD reactions in the preceding paper (1). An oxide catalyst sample containing 50 μmol of a main metal component (Mo in the cases of Mo, CoMo, WCM, or CWM catalyst series; W in the cases of W or CoW; Co in the case of Co catalyst) was loaded into the quartz reactor. In order to remove adsorbed impurities, the sample was heated to 500°C for 0.5 h in dry O_2 (Hanguk UHP grade) flow (30 cm^3/min) and maintained at this temperature for 0.5 h followed by cooling to 40°C. Then the oxygen flow was switched to a purified reductive gas mixture of 10% H_2 in Ar. After stabilization of the TCD signal, the temperature was increased at a rate of 15°C/min to 700°C and kept at this temperature for 0.5 h. H_2 concentration in the effluent stream was monitored with the TCD and the water produced during reduction was trapped with molecular sieve 13X.

UV-Vis DRS

The UV-Vis diffuse reflectance spectra of the oxidic state catalyst samples were recorded in the range of 200–700 nm, using a Shimazu 240 UV-Vis Diffuse Reflectance Spectrometer. A quartz cell capable of providing a sample thickness larger than 3 mm was employed, which permits the direct determination of $R\infty$, the reflectance at infinite sample thickness. The quartz cell containing the catalyst samples was first heated to 100°C and evacuated for 0.5 h to remove the physically adsorbed species. $BaSO_4$ was used as a reflectance white standard.

ESR

ESR spectra were recorded on a Brucker ESP 300 spectrometer with a single cavity at room temperature in the 2000–4500 G range. The working frequency was 9.75 GHz and the magnetic field was modulated at 100 kHz using an incident microwave power of 2 mW. A varian strong pitch sample ($g = 2.0028$) was used to calibrate g values (spectroscopic splitting factors). An ESR cell was specially designed so that catalyst samples sulfided in the quartz reactor could be transferred to the ESR cell without air contact. In order to remove the physically adsorbed species, the ESR cell was evacuated at 0.1 mmHg for 10 min at room temperature. The sulfidation of oxide catalyst samples (0.1 g) for ESR was performed in the same manner as used in HDS or HYD reaction.

XPS

XPS spectra were recorded with a Leybold, LHS-10 spectrometer equipped with a Mg$K\alpha$ X-ray excitation source operated at 100 mA and 10 kV. A powdered oxide catalyst sample was pressed into two thin wafers with 10 mm diameter, one of which was used for the oxidic state analysis and the other was sulfided according to the same procedure as for the previous HDS or HYD experiment (1) for the sulfided state analysis. After sulfidation the reactor was cooled to −78°C, using a cold bath of acetone and dry ice, and maintained at this temperature for 30 min in 30 cm^3/min flow of purified N_2. As soon as the reactor was opened in the upward flow of N_2, an adequate amount of isooctane (Aldridge, 99.7 + %), enough to soak the sulfided wafer, was injected into the reactor with a syringe. The wafer soaked with isooctane was immediately fixed to the XPS sample holder and evacuated down to 10^{-3} Pa before it was moved into the analysis chamber. It has been reported that cooling the fresh sulfided catalysts to low temperature (3) and coating with isooctane (4, 5) before their exposure to air is helpful in preventing their oxidation by air. The spectra of the Al2*s*, Mo3*d*, Co2*p*, W4*f*, and S2*p* levels were recorded. Binding energies were determined referred to the binding energy of Al 2*s* at 119.1 eV.

RESULTS

XRD

For the oxidic state catalysts of the CWM and WCM series and Co(1.71)Mo(4.0), no significant diffraction patterns attributable to the impregnated metal species appear. This indicates that the impregnated metal components are well dispersed on the support surface and do not form any XRD-detectable bulk species.

TPR

Figure 1 shows the TPR profiles of some base catalysts. The W(5.0) catalyst does not show any significant reduction peaks. This low reducibility of the alumina-supported W catalyst has been generally known (6–8) and interpreted as due to the polarizing effect of Al^{3+} ions of the support (6). The two small reduction peaks observed in the TPR profiles of Co(2.14)W(5.0), which was prepared by impregnating Co onto the W(5.0) catalyst, may be attributed to

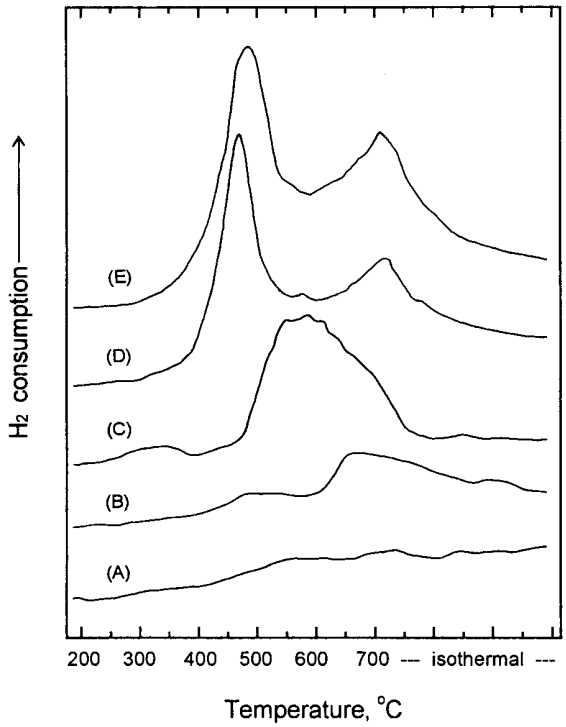

FIG. 1. TPR profiles of (A) W(5.0), (B) Co(2.14)W(5.0), (C) Co(4.0), (D) Mo(4.0), and (E) Co(1.71)Mo(4.0).

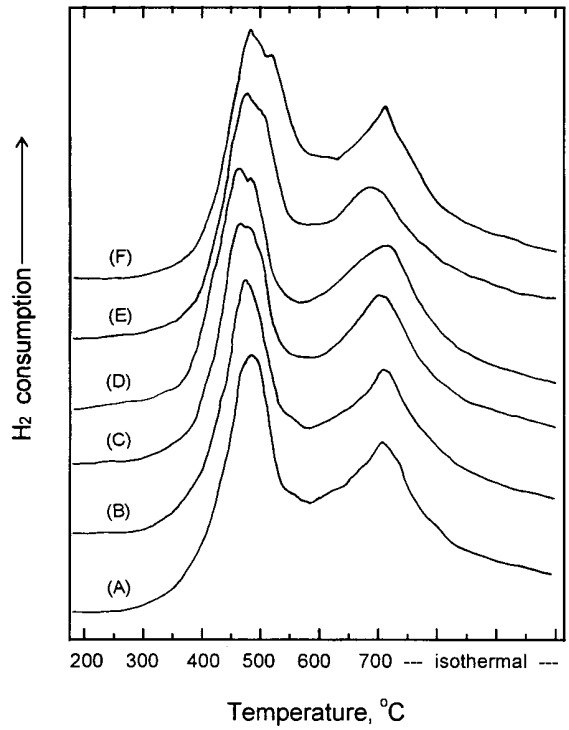

FIG. 2. TPR profiles of (A) Co(1.71)Mo(4.0) and CWM series catalysts containing tungsten in W/(W + Mo) atomic ratio as follows: (B) 0.0125, (C) 0.025, (D) 0.05, (E) 0.1, and (F) 0.2.

the reduction of Co species in view of the TPR profile of Co(4.0) exhibiting a broad reduction pattern starting at 450°C. The TPR profiles of Mo(4.0) and Co(1.71)Mo(4.0) catalysts resemble each other in the shape exhibiting the two reduction regions as reported (8–13). Medema *et al.* (9) proposed that two Mo species are present for Mo loading up to monolayer coverage (8): (i) isolated tetrahedral molybdenum-oxide (Mo_T), which is resistant to reduction, and (ii) ploymeric distorted octahedral molybdenum-oxide (Mo_o), which is easier to reduce. Several authors (9–13) suggested for the two-peak reduction pattern of Mo catalysts that the low-temperature reduction peak be assigned to the partial reduction of Mo_o and the high temperature peak to further reduction of such species plus that the Mo_T. However, the high-temperature reduction peak in the present experiments seems not to be related to reduction of Mo_T because these species require higher temperatures to become reduced than those currently employed.

The TPR profile of Co(1.71)Mo(4.0) catalyst shows the increase in the degree of reduction as compared with Mo(4.0). Such increase induced by Co impregnation might be originated from the reduction of Co species rather than the additional reduction of Mo species because the two catalyst samples have equal amounts of molybdenum. The Co-oxides in alumina supported catalysts are configured as tetrahedrally coordinated species, which are resistant to being reduced, and octahedrally coordinated species and bulk Co_3O_4, both of which are reducible (14). It is striking that the additional reduction has occurred evenly within the temperature region confined by the two reduction peaks of Mo(4.0). This indicates that the reducible Co-oxide species are present as forming Co–Mo–O phases (11, 14). That the Co–Mo–O structures are not much different from the original polymolybdate phases in Mo/Al_2O_3 could be a reason for the even increase of the TPR spctrum as compared to the unpromoted sample.

The TPR profiles of CWM series catalysts are presented in Fig. 2. It should be noted that the absolute amount of molybdenum in the samples has been kept constant (50 μmol of Mo), i.e., sample sizes are increased with increasing content of tungsten. The TPR profiles of all the catalysts containing tungsten display two reduction peaks similar to those of Co(1.71)Mo(4.0). However, general trends in the peak-width broadening towards the higher temperature region and small shifts of the maximum peak position are observed with increasing W-content. The width of the first reduction peak becomes broader as the content of tungsten increases and the maximum peak position is first shifted towards lower temperatures and then moved towards higher temperatures. However, the total amounts of reduction appear not to be greatly changed with the tungsten content. Similar trends were observed for the catalysts of WCM series based on the Co(1.71)Mo(4.0), although they are not

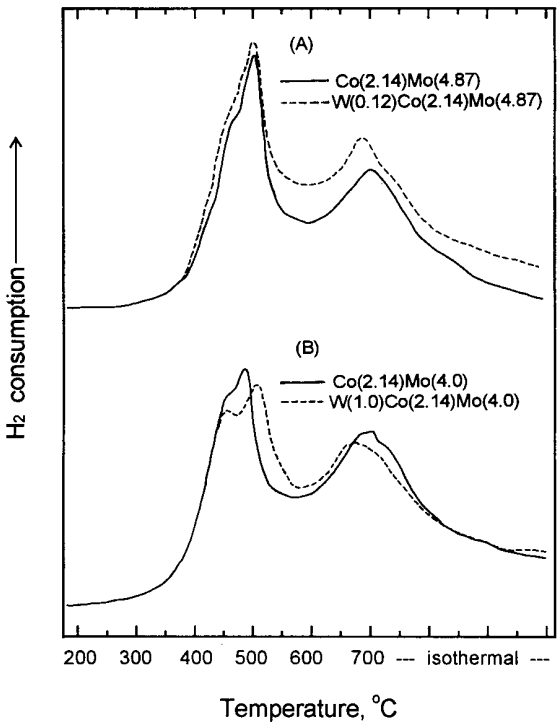

FIG. 3. TPR profiles of WCM-A catalysts, (A) Co(2.14)Mo(4.87) and W(0.12)Co(2.14)Mo(3.87), and (B) Co(2.14)Mo(4.0) and W(1.0)Co(2.14) Mo(4.0).

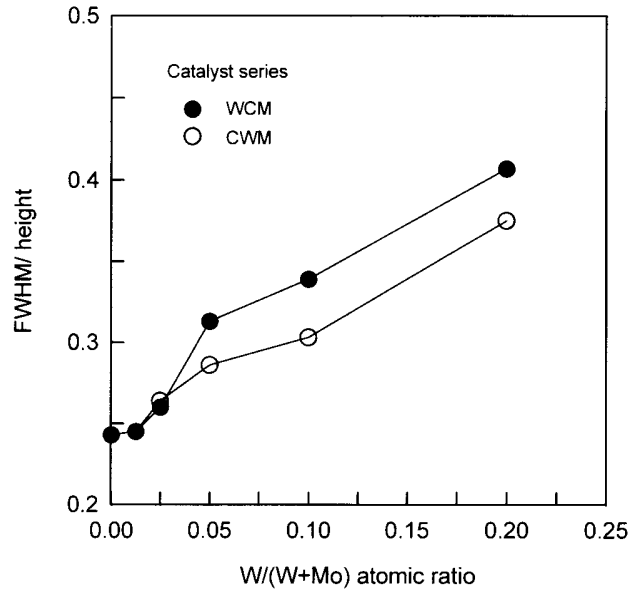

FIG. 4. The ratios of FWHM to the maximum height of the first peak of TPR profiles of the catalysts of Co(1.71)Mo(4.0), and CWM and WCM series.

presented here. Figure 3 shows the TPR profiles of WCM-A catalysts. The TPR profile of W(0.12)Co(2.14)Mo(4.87) compared with that of its base Co(2.14)Mo(4.87) shows higher amounts of reduction instead of a shift of the maximum peak position as observed in CWM and WCM series catalysts. It is presumed that W-oxides present in the W-incorporated catalysts experience almost no reduction according to the extremely low reducibility of the W(5.0) catalyst, as shown in Fig. 1A.

The shift of the maximum peak position towards lower temperatures observed in the relatively low W-content catalysts suggests that some of the Mo (or Co) species have been rendered more reducible by the presence of tungsten. It has been reported (11, 14) for the alumina-supported CoMo catalysts that Mo increases the Co reducibility. Arnoldy *et al.* (11) explained this influence of Mo on the Co reducibility, suggesting that the presence of Mo^{6+} ions in the Co surroundings results in a decreased number of Al^{3+} neighbors, decreasing the polarization of the Co–O bonds, and consequently resulting in a higher reducibility. Likewise, it is possible that the presence of W^{6+} ions in the Co or Mo surroundings lowers the number of Al^{3+} neighbors around Co or Mo ions, resulting in a better reducibility. Also the possibility cannot be excluded that WO_3 species are placed or intercalated between the isolated monomeric Mo_T species and, as a result, the monomeric Mo_T species is bridged via W^{6+}-linked oxygen to form a structure similar to the octahedral coordination. Such a postulation was reported (9, 14) for the alumina-supported Mo catalysts, that is, when the Mo impregnation level is increased, the isolated monomeric Mo_T is bridged by oxygen to form ploymeric Mo in octahedral coordination.

The peak-width broadening towards higher temperatures without a significant change in the total peak area indicates that the retardation occurred in the rate of reduction of the corresponding reducible species. In order to evaluate such peak-width broadening with the tungsten content, the ratios of FWHM (full width at half maximum) to the maximum height of the first peak are shown in Fig. 4. The effects of retardation on the reduction by tungsten appear not so large as to be neglected in cases with lower tungsten content but become more and more significant with higher contents of tungsten. On the whole, such effects are more pronounced in the catalysts of the WCM series than the CWM series.

From the above results, it can be stated that the tungsten incorporated in CoMo catalysts affects the reduction behavior of the catalyst in two complicated ways, i.e., a small shift of the peak maximum position to lower temperatures and the retardation of the overall reduction rate, depending on its content. In the relatively low content of tungsten, the former as a favorable effect is pronounced without a significant effect of the latter, while in the higher content of tungsten the latter effect prevails against the former.

DRS

DRS spectra of the CWM series catalysts as well as Co(1.71)Mo(4.0) are presented in Fig. 5. All catalysts show

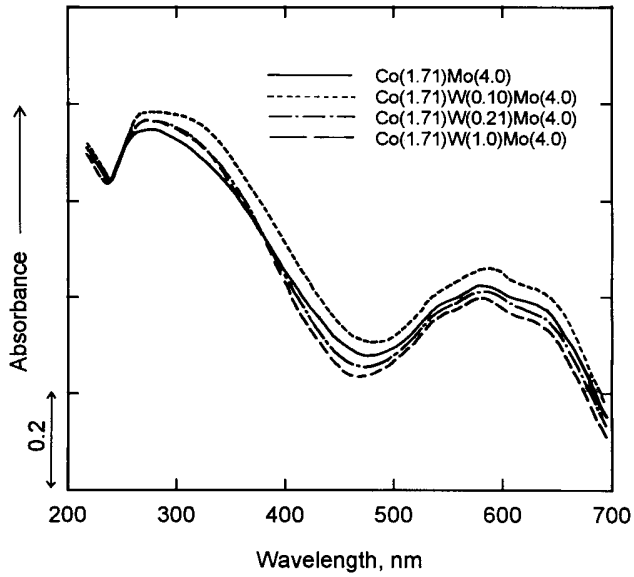

FIG. 5. DRS spectra of CWM series catalysts and Co(1.71)Mo(4.0).

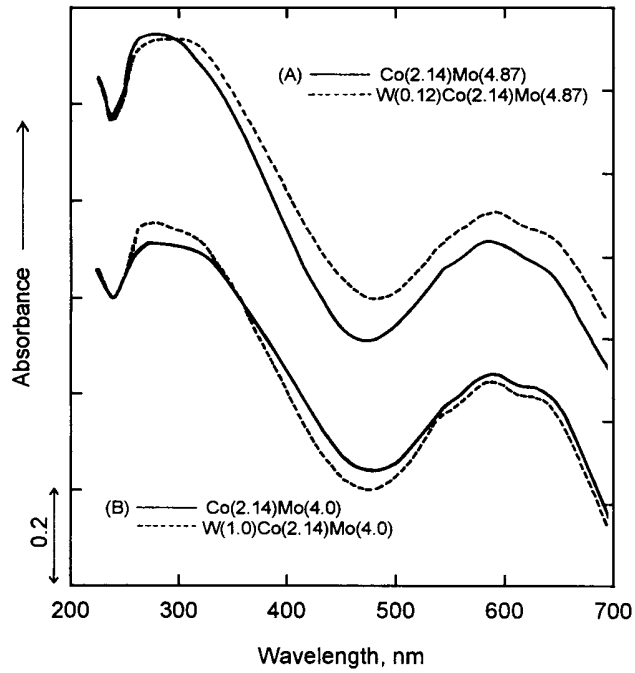

FIG. 6. DRS spectra of WCM-A catalysts, (A) Co(2.14)Mo(4.87) [0.957] and W(0.12)Co(2.14)Mo(4.87) [1.011], and (B) Co(2.14)Mo(4.0) [0.992] and W(1.0)Co(2.14)Mo(4.0) [0.974], where the bracketed numbers indicate the absorbance ratio, $F(R\infty)_{320}/F(R\infty)_{260}$, of the spectra.

similar spectra, exhibiting one broad band at about 300 nm and triplets centered at about 583 nm. The DRS spectra of WCM series catalysts, although not presented here, shows patterns similar to those of CWM series catalysts. The band appearing at 250–350 nm in the present catalysts indicates the presence of Mo^{6+} species in tetrahedral and octahedral coordination. According to the literature (14–17), the bands at the lower wavelength region (220–270 nm) and that at the higher wavelength region (300–330 nm) are due to isolated tetrahedral MoO_4^{2-} species (Mo_T) and octahedral Mo^{6+} (Mo_o), respectively. The triple bands centered at 583 nm are reported (14, 16, 18) to represent tetrahedrally coordinated Co^{2+} species.

The position of the Mo band maximum is not significantly changed with the W content. However, the band is shifted or broadened slightly towards the octahedrally coordinated Mo^{6+} region in Co(1.71)W(0.1)Mo(4.0), of which W-composition corresponds to 0.025 W/(W + Mo). Similar Mo band broadening towards the high wavelength region is observed also for the catalyst W(0.12)Co(2.14)Mo(4.87), as shown in Fig. 6A. However, catalysts containing tungsten at the higher contents are less broadened than Co(1.71)W(0.1)Mo(4.0), as shown in Figs. 5 and 6B. Such minor broadening at higher contents of tungsten might be originated from the presence of tetrahedrally coordinated W^{6+} species covering the molybdate surface in higher population. W(5.0) supported on Al_2O_3 shows a single band at about 260 nm, which is attributed to tetrahedrally coordinated W^{6+} species (19), as shown in Fig. 7A, indicating that the catalyst consisted mainly of the tetrahedrally coordinated W^{6+} species. The impregnation of tungsten was done at pH 9.5, in which tetrahedral WO_4^{2-} anions are the predominant species (20–22). As shown in Fig. 7, the intro-

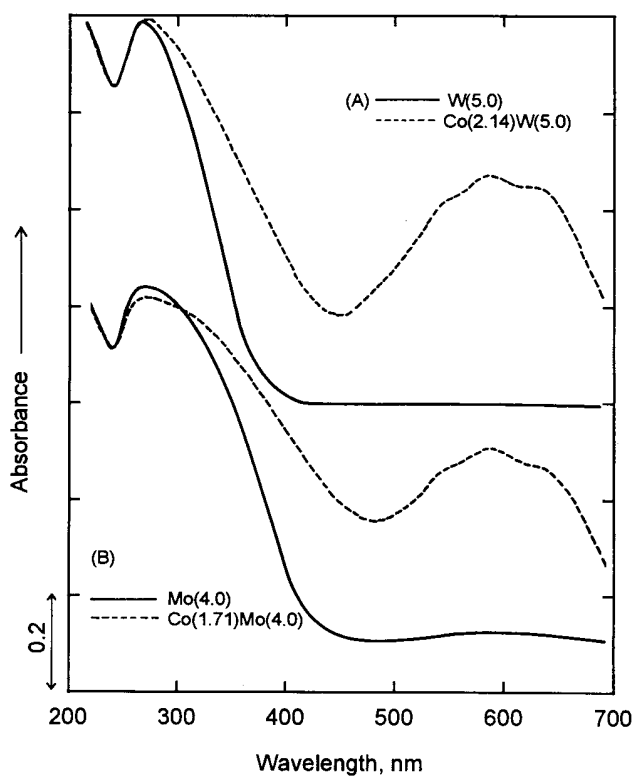

FIG. 7. DRS spectra of (A) W(5.0) and Co(2.14)W(5.0), and (B) Mo(4.0) and Co(1.71)Mo(4.0).

duction of Co to Mo or W catalyst leads to a shift of the Mo or W band towards higher wavelength region, indicating a change in the Mo or W coordination to the octahedral.

In order to estimate the relative contribution of the oxidic Mo species in the W-incorporated catalysts, the ratios of $F(R\infty)_{320}/F(R\infty)_{260}$, which indicate the relative concentrations of Mo_o to Mo_T, are shown in Fig. 8. Although the ratios are varied within a narrow range, it can be observed that increasing the W content in the catalysts gives a maximum in the relative fraction of Mo_o at 0.025 W/(W + Mo), and that the relative Mo_o fractions are higher for the WCM series catalysts than the CWM series catalysts at the same W-content. These results indicate that the incorporation of tungsten leads to a relative decrease in Mo_T and an increase in Mo_o species, and that such an effect is maximized for the catalyst of tungsten content corresponding to 0.025 W/(W + Mo).

The spectra in the wavelength region 500–700 nm are different from each other in their band intensities with increasing tungsten content, as shown in Figs. 5 and 6. The W-incorporated catalyst Co(1.71)W(0.1)Mo(4.0) or W(0.12)Co(2.14)Mo(4.87), which corresponds to 0.025 W/(W + Mo), exhibits higher band intensity than the reference CoMo catalysts, while the band intensities of the catalysts containing W at higher content are comparatively lower. According to previous reports (23, 24) indicating that the signal due to the octahedrally coordinated Co^{2+} species (Co_o) overlaps with the broad triplet of tetrahedrally coordinated Co^{2+} species (Co_T), it is difficult to conclude that the increase in the band intensity is attributed to the increase in the Co_T resulting from the decrease in Co_o, or *vice versa*. Consequently, it can be thought that the increase or decrease in the band intensity is due to the increase or decrease in the surface density of Co species regardless of its coordination.

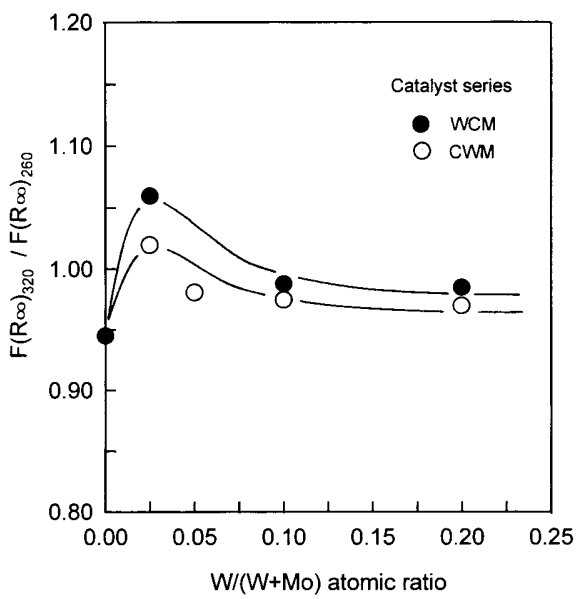

FIG. 8. $F(R\infty)_{320}/F(R\infty)_{260}$ of sulfided CWM and WCM series catalysts versus tungsten content.

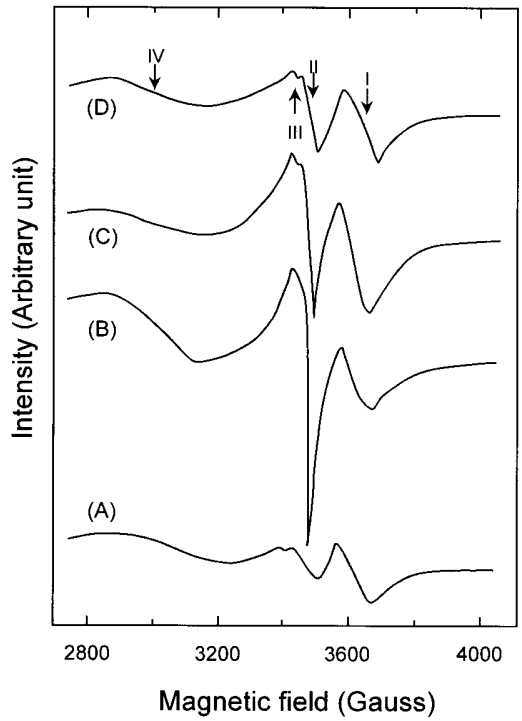

FIG. 9. ESR spectra of sulfided WCM series catalysts, (A) Co(1.71)Mo(4.0), (B) W(0.1)Co(1.71)Mo(4.0), (C) W(0.44)Co(1.71)Mo(4.0), and (D) W(1.0)Co(1.71)Mo(4.0).

ESR

The ESR spectra of the sulfided WCM series catalysts as well as Co(1.71)Mo(4.0) are presented in Fig. 9. Four ESR bands appeared at *g* values of 1.93 (band (I)), 2.0 (band (II)), 2.04 (band (III)), and 2.31 (band (IV)). Band (I) can be assigned to oxo-Mo^{+5} interacting with the alumina support (25–29) and band (II) to Mo species in sulfur environments, i.e., bulk defects in a MoS_2-like phase or Mo^{3+} ions connected with anion vacancies, which are directly related to catalytic activity (25–27). Because the paramagnetic properties of W are not much different from those of Mo (25–27), bands (I) and (II) could also arise from tungsten. Band (III), with relatively low intensity, can be assigned to sulfur radical species according to ESR studies (25–27) reporting that the band attributed to the sulfur radical species on MoS_2 or WS_2 consisted of triplet bands of *g* values centered at 2.04. From the viewpoint of its broadeness, band (IV), appearing at a *g* value of about 2.31, suggests the presence of species of strong ferromagnetic character. In the ESR study on unsupported NiW catalysts, Thakur *et al.* (26, 27) reported a broad band at a *g* value of 2.32, similar to band (IV). They suggested that this band originated from the presence of

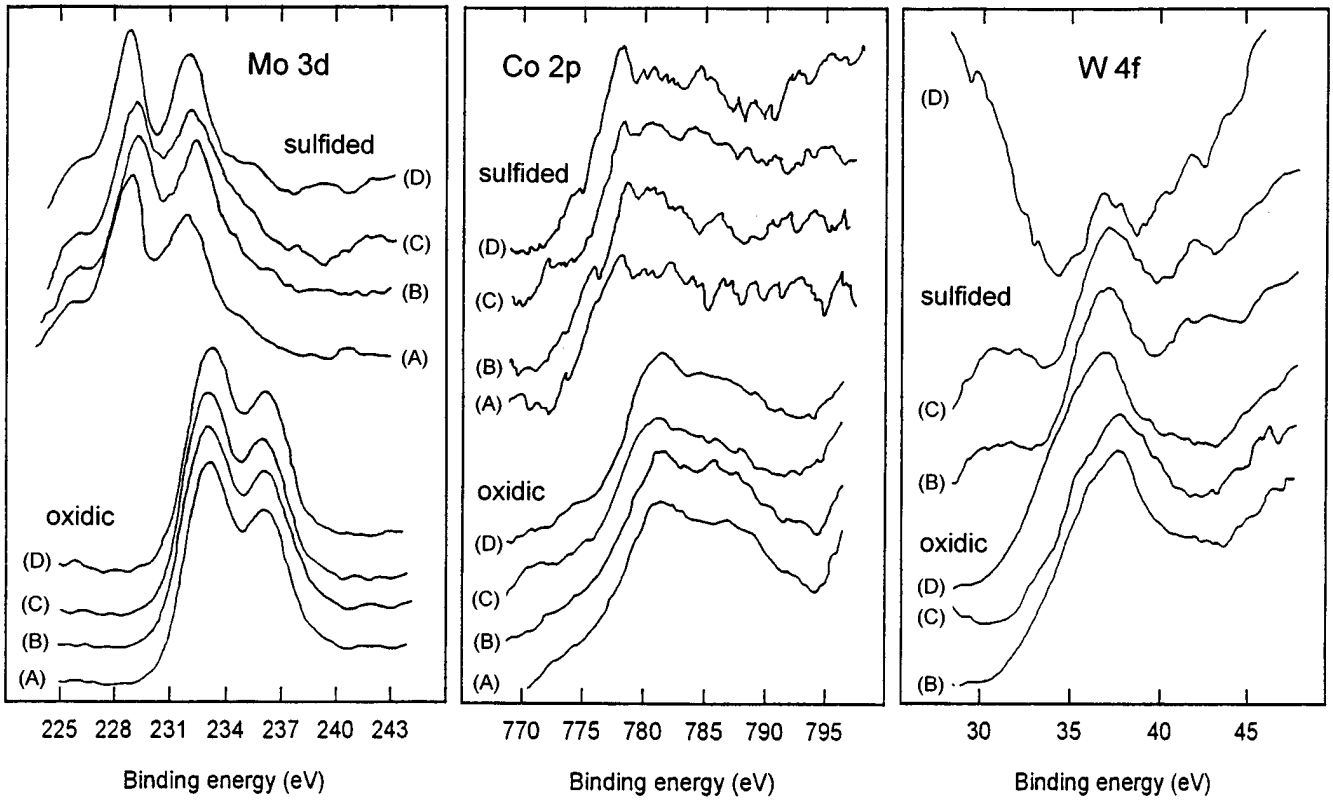

FIG. 10. XPS spectra of Mo3*d* (left), Co2*p* (center), and W4*f* (right) for the catalysts (A) Co(1.71)Mo(4.0), (B) W(0.1)Co(1.71)Mo(4.0), (C) Co(1.71)W(0.1)Mo(4.0), and (D) Co(1.71)W(1.0)Mo(4.0) in their sulfided (upper) and oxidic (lower) states.

some ferromagnetic nickel sulfide. They found that HDS and HYD activities of the catalysts were related to the intensity of the ESR band of ferromagnetic nickel sulfide and suggested that the interaction between the ferromagnetic nickel sulfide and W^{3+} present in WS_2 was responsible for the increased activity. The band (IV) might be assigned to ferromagnetic cobalt species in our case.

As it can be seen from Fig. 9, the intensities of the ESR bands (I), (II), and (IV) are strongly dependent on the content of tungsten incorporated. The intensity of band (I) increases more or less with increasing content of tungsten, while that of band (II) or band (IV) increases extremely for the catalyst W(0.1)Co(1.71)Mo(4.0) of 0.025 W/(W + Mo) and decreases with further increases in tungsten content. The increases in band (I) intensity with increasing tungsten content may be originated from the partial sulfidation of W^{6+} to W^{5+} or may be due to the retardation effects on the reduction of Mo oxide by tungsten present in higher content, as ascertained by TPR (Fig. 4). Band (II) is thought to be mainly originated from molybdenum, considering the extremely low reducibility of tungsten oxide supported on alumina. The trends observed in the intensity changes of bands (II) and (IV) with tungsten content are quite analogous to those of HDS and HYD activities, and oxygen uptake as reported elsewhere (1). These ESR results also ascertain that the presence of tungsten to an appropriate amount in CoMo catalyst facilitates the creation of Mo^{3+} ions which play the role of catalytic active centers.

XPS

The XPS spectra of Mo3*d*, Co2*p*, and W4*f* for the catalysts of Co(1.71)Mo(4.0), W(0.1)Co(1.71)Mo(4.0), Co(1.71)W(0.1) Mo(4.0), and Co(1.71)W(1.0)Mo(4.0) in their oxidic and sulfided states are shown in Fig. 10. The binding energy (BE) data are summarized in Table 1.

The spectra and the BE data for Mo3*d* and Co2*p* of the oxidic state catalysts show that the BE values are not significantly altered by the incorporation of tungsten in a low content but increase considerably with the tungsten in a high content. On the other hand, for the sulfided state catalysts, the BEs of Mo and Co are considerably increased by the presence of tungsten for W(0.1)Co(1.71)Mo(4.0) and Co(1.71)W(0.1)Mo(4.0). However, such increase is not observed for Co(1.71)W(1.0)Mo(4.0). The increases in BE in the sulfided state indicate the increase in the dispersion of the sulfided phases of Mo and Co (30). The BE value of W4*f* in oxidic catalysts of low W-loading is higher than that of high W-loading. The Mo3*d* spectra show that most of molybdenum oxide species are converted to the sulfided

TABLE 1

XPS Binding Energy Data for the Catalysts in Oxidic and Sulfided States

Catalysts	Mo3$d_{5/2}$	Mo3$d_{3/2}$	Co2$p_{3/2}$	W4f	S2p	$\Delta(BE)_1$[a]	$\Delta(BE)_2$[b]
In oxidic state							
Co(1.71)Mo(4.0)	233.0	236.0	781.2	—			
W(0.1)Co(1.71)Mo(4.0)	233.0	236.0	781.1	37.7			
Co(1.71)W(0.1)Mo(4.0)	232.9	235.9	781.1	37.6			
Co(1.71)W(1.0)Mo(4.0)	233.4	236.4	781.5	37.0			
In sulfided state							
Co(1.71)Mo(4.0)	228.8	231.8	778.7	—	162.1	66.7	616.6
W(0.1)Co(1.71)Mo(4.0)	229.4	232.5	778.9	37.0	162.4	67.0	616.5
Co(1.71)W(0.1)Mo(4.0)	229.1	232.1	778.5	37.0	162.2	67.0	616.3
Co(1.71)W(1.0)Mo(4.0)	228.6	231.8	778.3	36.7	162.1	66.5	616.2

[a] $\Delta(BE)_1$, binding energy difference, Mo3$d_{5/2}$-S2p.
[b] $\Delta(BE)_2$, binding energy difference, Co2$p_{3/2}$-S2p.

species by the sulfidation, but a small amount of molybdenum still remains oxidic after the sulfidation. The increased broadeness of the Co2p spectra in sulfided samples points to the presence of Co species both in sulfided and oxidized forms after the sulfidation (31). The sulfiding-resistant Co-oxides are supposed to be tetrahedrally coordinated species. It can be observed from the W4f spectra that most of the tungsten oxides of W(0.1)Co(1.71)Mo(4.0) and Co(1.71)W(0.1)Mo(4.0) catalysts remain oxidic after the sulfidation and that, on the other hand, larger amounts of tungsten oxides have been converted to the sulfides in the Co(1.71)W(1.0)Mo(4.0) catalyst.

Alstrup *et al*. (32) proposed the use of the BE differences of (Mo3$d_{5/2}$–S2p) and (Co2$p_{3/2}$–S2p) as a reliable way to identify the sulfided species of Mo and Co. Table 1 gives the values of such BE differences, $\Delta(BE)_1$ and $\Delta(BE)_2$, for ($Mo_3d_{5/2}$–S2p) and (Co2$p_{3/2}$–S2p), respectively. The mean value of $\Delta(BE)_1$, 66.8 eV, corresponds closely to the value 66.9 eV reported for MoS_2 by Alstrup *et al*. (32). The $\Delta(BE)_2$ values, 616.6 and 616.5 eV, for Co(1.71)Mo(4.0) and W(0.1)Co(1.71)Mo(4.0) catalysts, respectively, are reasonably close to the value 617.0 eV, which is reported to be characteristic of Co in the CoMoS phase (32), as ascertained by Bouwens *et al*. (33). On the other hand, the $\Delta(BE)_2$ values for the CWM series catalysts of Co(1.71)W(0.1)Mo(4.0) and Co(1.71)W(1.0)Mo(4.0), 616.3 and 616.2 eV, respectively, are closer to 616.1 eV, which is typical for Co_9S_8 (32), rather than to 617.0 eV, for Co in CoMoS phase. The value of S2p BE, 162.1 eV, indicates the presence of S^{2-} on the sulfided catalyst surface (32, 34).

DISCUSSION

Structure of the CoMo Catalyst

From the TPR and DRS results for the Mo and CoMo base catalysts in this study, it is assured that the most probable Mo-oxide species in the oxidic state catalysts are isolated Mo_T and polymeric Mo_o. The introduction of Co to the Mo catalyst induces some changes in the Mo-oxide structure from tetrahedral to octahedral, as indicated by DRS spectra. The TPR results indicate that the reducible Co-oxide species in the CoMo catalyst are well distributed, associated as Co–Mo–O phases, which have been known as the precursors of highly active Co–Mo–S (35–37). The existence of the Co–Mo–S phase in the sulfided Co(1.71)Mo(4.0) catalyst is verified by the BE difference in XPS analysis. However, the DRS result indicates that nonreducible Co_T species are also present in a significant amount. It has been reported that the Co-promoted Mo catalysts are preferentially present as a monolayer on the alumina support (38, 39).

Effects of Impregnation Order and Tungsten Content

Throughout the interpretation of the characterization results in the preceding section, the textural and structural effects induced by the incorporation of tungsten in CoMo catalyst are found to be dependent on the impregnation procedure and the loading content of tungsten. As shown in Table 1 of (1), the textural effect, which is exemplified by the changes in surface area, is generally considered to be not so significant to induce large differences in the reaction rates. The surface areas of the catalysts slightly decrease with increasing tungsten content, indicating that the impregnated metal oxides have been well dispersed on the catalyst surface without the formation of large bulk-like species which may block the fine pores of the alumina support. The absence of bulk species is also corroborated by XRD results. However, the structural effects exerted by tungsten incorporation induced the changes in catalytic activity. A simplified description for the structural changes of tricomponent catalysts affected by the tungsten impregnation sequence and its loading is presentedin Fig. 11.

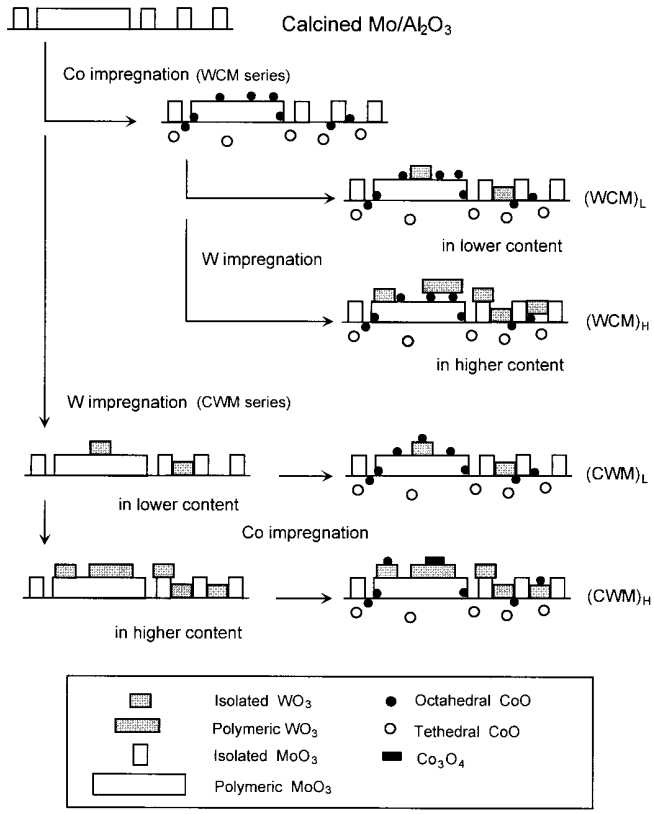

FIG. 11. Simplified description for the trimetallic catalysts prepared by impregnating a fixed amount of Co and variable amount of W onto the Mo/γ-Al_2O_3 with alternation in the impregnating sequence of cobalt and tungsten.

W-Impregnation onto CoMo/γ-Al_2O_3

The most distinct feature of this case is that tungsten is impregnated onto the catalyst in which relatively large fractions of both Co and Mo have been chemically associated with each other as Co–Mo–O phases. In the low content of tungsten up to 0.025 W/(W + Mo), as shown as $(WCM)_L$ in Fig. 11, monomeric oxide species of tungsten in the calcined catalyst may result in the preferential formation of a bond with alumina, occupying the Mo or Co oxide-free vacant sites, and some of the species may be also placed on top of the polymeric Mo_o monolayer which has been associated with cobalt atoms. At this amount of tungsten incorporation, the catalytic activities of HDS and HYD are maximum, which can be explained by the results obtained from the various characterization methods as follows: (i) TPR, shift in the first TPR peak towards lower temperature, (ii) DRS, maximal increase in the ratios of Mo_o/Mo_T (iii) ESR, maximal increase in the band intensity of Mo^{3+} ions, and (iv) XPS, increase in the BE values of the sulfided Mo, indicating its increased dispersion. In addition, a sharp increase in the O_2 uptake of the catalysts was previously reported (1). Within this low content of tungsten, it is also assured from the XPS results that Co–Mo–O phases previously formed are mostly preserved, resulting in Co–Mo–S phases after sulfidation.

At a high content of tungsten, as shown as $(WCM)_H$ in Fig. 11, larger fractions of Co- and Mo-oxides surface may be covered with W-oxide. As a result, phenomena such as the peak-width broadening and the shift of the TPR peak towards higher temperatures become prominent. The BE values of Mo- and Co-oxides increase. These are the adverse effects of tungsten on the sulfidation of oxide precursors and on the catalytic activity. Due to the higher population of W-oxides on the surface, the previously existing Co–Mo–O phases may be dissociated to form Co–W–O phase, which results in the oxidic precursor of less active Co–W–S phases (40). A large portion of Co–Mo–O structures of W(1.0)Co(1.71)Mo(4.0) catalyst is considered to be damaged, leading to the formation of Co–W–O structures. As discussed in (1), this is suggested by the facts that the catalytic properties of W(1.0)Co(1.71)Mo(4.0) were closer to the CWM series rather than the WCM series, as shown in the correlation of the HDS and HYD activities with oxygen uptake.

W-Impregnation onto Mo/γ-Al_2O_3 Prior to Co-Impregnation

In this case, tungsten was impregnated onto Mo/γ-Al_2O_3 before impregnating cobalt. Cobalt has a higher probability to become associated with W-oxides which are present on the surface of support or on Mo-oxide layers, resulting in the formation of less active Co–W–O phases instead of more active Co–Mo–O. However, at a lower content of tungsten, as shown as $(CWM)_L$ in Fig. 11, the same favorable effects as discussed above are predominant over the unfavorable effects in the Co–W–O phase formation. The effect of W-incorporation on the creation of the active sites on MoS_2 is likely to be more effective in this $(CWM)_L$ catalyst than in the $(WCM)_L$ catalyst because oxygen uptakes are larger for the CWM series catalyts than for the WCM series, as shown in Fig. 3 of (1).

At a higher content of tungsten, an increase is expected in the fraction of W-covered surface of the Mo/γ-Al_2O_3 and, accordingly in the number of Co–W–O phases which will bring about unfavorable effects on the catalytic activity to a great extent. Part of the cobalt impregnated next may produce a small amount of bulk oxide, Co_3O_4, which is a precursor of Co_9S_8, due to the scarcity of adsorption sites on the surface of Mo-oxide and the support, as ascertained by XPS.

Role of Tungsten as a Promoter for CoMo/γ-Al_2O_3

The promotion in the activity of CoMo/γ-Al_2O_3 by the addition of small amount of tungsten can be explained by the results obtained from various characterization methods, i.e., change of Mo_T to Mo_o (DRS), the increase in the reducibility of Mo or Co oxide species (TPR), more

creation of active sites on MoS_2 phase (ESR), and increase in the dispersion of MoS_2 phase (XPS). Such favorable characterizing evidence is more clearly detected for the sulfided catalysts than the oxidic catalysts. Actually, XPS analysis (Fig. 10 and Table 1) for the oxidic state catalysts shows no substantial differences between the base catalyst of Co(1.71)Mo(4.0) and the catalyst of W(0.1)Co(1.71)Mo(4.0) or Co(1.71)W(0.1)Mo(4.0), notwithstanding the differences in the catalytic activities between the catalysts that apparently exist, as reported in (1). This indicates that the small amount of tungsten did not significantly affect the oxidic precursors but affected greatly the state of sulfides. The number of active sites are dependent on the dispersion of MoS_2 because highly dispersed MoS_2 phases can provide more sites on their edges (39, 40). These results suggest that the monomeric W-oxides play a certain deterministic role, which is related to the dispersion of sulfided Mo phase during sulfidation. The comparison of XPS spectra of Mo3*d* with W4*f* reveals that W-oxides have been sulfided to a slight extent, while Mo-oxides have been to a nearly complete extent. It has been reported (29) that the sulfidation of $CoMo/Al_2O_3$ catalysts to a complete extent facilitates the formation of crystalline molybdenum sulfide, resulting in the decrease of dispersion. It can be thought that this sulfiding-resistant WO_4^{-2} contributes to increasing or at least maintaining the dispersion of MoS_2 layers and thereby providing more affordable active sites.

CONCLUSION

The promotional effect obtained by the addition of a small amount of tungsten to $CoMo/\gamma\text{-}Al_2O_3$ was attributed to the positive roles of tungsten as follows: (i) changing the Mo-oxide coordination from tetrahedral to octahedral, (ii) facilitating the reduction of Mo-oxide species, and (iii) increasing the dispersion of MoS_2, which lead to the increased number of coordinatively unsaturated sites during sulfidation. By incorporating tungsten at a content as much as 0.025 in W/(W + Mo) atomic ratio, the MoS_2 dispersion of $CoMo/\gamma\text{-}Al_2O_3$ catalyst was considered to be maximized without noticible detriment to the active Co–Mo–O phase. At this content of tungsten, cobalt was characterized to be mainly involved in the active Co–Mo–S phase. Such effects of tungsten on the dispersion of active phase was not much different between the catalyst series WCM and CWM but the formation of active Co–Mo–O phases more favored in the WCM series than in the CWM series. The decrease in activity observed in the catalysts containing higher content of tungsten was originated from the increase in the W-oxide coverage on the surface of Mo-oxides or Co–Mo–O phases. It was understood that the increased coverage of W-oxides on the surface of such active phase precursors resulted in not only impeding the reduction or sulfidation of the oxidic precursor but also facilitating the formation of less active Co–W–O at the sacrifice of more active Co–Mo–O phase.

ACKNOWLEDGMENT

This work was supported by the Ministry of Trade, Industry and Energy, Republic of Korea.

REFERENCES

1. Lee, D. K., Lee, I. C., Park, S. K., Bae, S. Y., and Woo, S. I., *J. Catal.* **159**, 212 (1996).
2. Prins, R., De Beer, V. H. J., and Somorjai, G. A., *Catal Rev. Sci. Eng.* **31**, 1 (1989).
3. Shang, D. Y., Adnot, A., Kaliaguine, S., and Chmielowiec, J., *Can. J. Chem. Eng.* **71**, 725 (1993).
4. Cambra, J. F., Arias, P. L., Gumez, M. B., Legarreta, J. A., and Fierro, J. L. G., *Ind. Eng. Chem. Res.* **30**, 2365 (1991).
5. Papadopoulou, C., Lycourghiotis, A., Grange, P., and Delmon, B., *Appl. Catal.* **38**, 255 (1988).
6. Scheffer, B., Molhoek, P., and Moulijn, J. A., *Appl. Catal.* **46**, 11 (1989).
7. Cordero, R. L., Solis, J. R., Ramos, J. V. G., Patricio, A. B., and Agudo, A. L., "Proceedings, 10th International Congress on Catalysis, Budapest, 1992" (L. Guczi, F. Solymosi, and P. Tetenyi, Eds.), p. 1927. Akadémiai Kiadó, Budapest, 1993.
8. Thomas, R., Van Oers, E. M., De Beer, V. H. J., Medema, J., and Moulijn, J. A., *J. Catal.* **76**, 241 (1982).
9. Medema, J., Van Stam, C., De Beer, V. H. J., Konings, A. J. A., and Koningsburger, D. C., *J. Catal.* **53**, 386 (1978).
10. Brito, J. L., and Laine, J., *J. Catal.* **139**, 540 (1993).
11. Arnoldy, P., Franken, M. C., Scheffer, B., and Moulijn, J. A., *J. Catal.* **96**, 381 (1985).
12. Lopez Cordero, R., Gil Llambias, F. J., and Lopez Agudo, A., *Appl. Catal.* **74**, 125 (1991).
13. Rajagopal, S., Marini, H. J., Marzari, J. A., and Miranda, R., *J. Catal.* **147**, 417 (1994).
14. Chung, K. S., and Massoth, F. E., *J. Catal.* **64**, 320 (1980).
15. Fournier, M., Louis, C., Che, M., Chaquin, P., and Masure, D., *J. Catal.* **119**, 400 (1989).
16. Ramirez, J., Cuevas, R., Gasque, L., Vrinat, M., and Breysse, M., *Appl. Catal.* **71**, 351 (1991).
17. Praliaud, H., *J. Less-Common Met.* **54**, 387 (1977).
18. De Beer, V. H. J., Van der Aalst, M. J. M., Machieels, C. J., and Schuit, G. C. A., *J. Catal.* **43**, 78 (1976).
19. Scheffer, B., Heijeinga, J. J., and Moulijn, J. A., *J. Phys. Chem.* **91**, 4572 (1987).
20. Tytko, K.-H., and Glemser, O., *Adv. Inorg. Chem. Radiochem.* **19**, 239 (1976).
21. Baes, C. F., and Mesmer, R. E., "The Hydrogenolysis of Cations," pp. 257–260. Wiley, New York, 1976.
22. Maitra, A. M., Cant, N. W., and Trimm, D. L., *Appl. Catal.* **27**, 9 (1986).
23. Vladov, C., Petrov, L., Ytua, B., and Topalova, L., *Appl. Catal. A: Gen.* **94**, 205 (1993).
24. Moon, S. J., Jeon, G. S., and Ihm, S. K., *HWAHAK KONGHAK* **26**, 617 (1988).
25. Konings, A. J. A., Brentjens, W. L. J., Koningsburger, D. C., and De Beer, V. H. J., *J. Catal.* **67**, 145 (1981).
26. Thakur, D. S., and Delmon, B., *J. Catal.* **91**, 308 (1985).
27. Thakur, D. S., Grange, P., and Delmon, B., *J. Catal.* **91**, 318 (1985).
28. Derouane, E. G., Petersen, E., Clausen, B. S., Gabelica, Z., Candia, R., and Topsoe, H., *J. Catal.* **99**, 253 (1986).
29. Kim, S. I., and Woo, S. I., *Appl. Catal.* **74**, 109 (1991).
30. Matralis, H. K., Lycourghiotis, A., Grange, P., and Delmon, B., *Appl. Catal.* **38**, 273 (1988).

31. Bouwens, S. M. A. M., Van Deer Kraan, A. M., De Beer, V. H. J., and Prins, R., *J. Catal.* **128**, 559 (1991).
32. Alstrup, I., Chorkendorff, I., Candia, R., Clausen, B. S., and Topsoe, H., *J. Catal.* **77**, 397 (1982).
33. Bouwens, S. M. A. M., Van Zon, F. B. M., Van Dijk, M. P., Van Deer Kraan, A. M., De Beer, V. H. J., Van Veen, J. A. R., and Koningsberger, D. C., *J. Catal.* **146**, 375 (1994).
34. Brown, J. R., and Ternan, M., *Ind. Eng. Chem. Prod. Res. Dev.* **23**, 557 (1984).
35. Topsoe, H., Clausen, B. S., Candia, R., Wivel, C., and Morup, S., *J. Catal.* **68**, 433 (1981).
36. Wivel, C., Candia, R., Clausen, B. S., Morup, S., and Topsoe, H., *J. Catal.* **68**, 453 (1981).
37. Topsoe, N.-Y., and Topsoe, H., *J. Catal.* **84**, 386 (1993).
38. Kemp, R. A., Ryan, R. C., and Smegal, J. A., "Proceedings, 9th International Congress on Catalysis, Calgary, 1988" (M. J. Phillips and M. Ternan, Eds.), Vol. 1, p. 128. Chem. Institute of Canada, Ottawa, 1988.
39. Eijsbouts, S., Heinerman, J. J. L., and Elzerman, H. J. W., *Appl. Catal.* **105**, 53 (1993).
40. Nag, N. K., Rao, K. S. P., Chary, K. V. R., Rao, B. R., and Subrahmanayam, V. S., *Appl. Catal.* **41**, 165 (1988).